Available online at www.sciencedirect.com
SCIENCE DIRECT®
Surface Science 566–568 (2004) 740–745
SURFACE SCIENCE
www.elsevier.com/locate/susc

The influence of surface defects on methanol decomposition on Pd(1 1 1) studied by XPS and PM-IRAS

O. Rodríguez de la Fuente, M. Borasio, P. Galletto, G. Rupprechter *, H.-J. Freund

Department of Chemical Physics, Fritz-Haber-Institut der MPG, Faradayweg 4-6, D-14195 Berlin, Germany

Available online 19 June 2004

Abstract

Methanol adsorption/desorption and its time- and temperature-dependent decomposition on well-annealed and defect-rich (ion-bombarded) Pd(1 1 1) were examined by X-ray photoelectron spectroscopy (XPS) and polarization-modulation infrared reflection absorption spectroscopy (PM-IRAS). Annealing CH_3OH multilayers from 100 to 700 K mainly resulted in CH_3OH desorption. Dehydrogenation to CO was a minor path and only trace amounts of carbon or carbonaceous species (CH_x; $x = 0$–3) were produced, i.e. C–O bond scission was very limited. By contrast, an exposure of 5×10^{-7} mbar CH_3OH at 300 K produced CH_x (~0.3 ML) on both surfaces but the rate of formation was not considerably enhanced by surface defects. On well-annealed Pd(1 1 1) isolated carbon atoms were identified by XPS in the early stages of carbon deposition, with carbon diffusion leading to the growth of carbon clusters in the later stages. Since carbon(aceous) species may either originate from C–O bond scission within methanol (or CH_xO) or from a consecutive dissociation of the dehydrogenation product CO, analogous experiments were also carried out with CO. PM-IRAS spectra up to 170 mbar CO, acquired using a UHV-high-pressure cell, did not show any indications of CO dissociation, excluding CO as source of carbonaceous deposits.

Keywords: Alcohols; Carbon monoxide; Palladium; X-ray photoelectron spectroscopy; Vibrations of adsorbed molecules; Catalysis; Low index single crystal surfaces

1. Introduction

Methanol adsorption/desorption and, in particular, methanol decomposition on noble metals has been the subject of many surface-analytical studies in the past (e.g. [1–4] and references therein). Methanol decomposition to CO and H_2 on Pd catalysts may provide a valuable source of hydrogen, e.g. for hydrogen-driven vehicles. However, catalyst deactivation by carbon deposits represents a serious limitation of this process. Consequently, one frequently discussed question is the probability of O–H versus C–O bond scission, resulting in CO and H_2, and in carbon or carbonaceous species (in the following denoted CH_x; $x = 0$–3), CH_4 and H_2O as products, respectively.

* Corresponding author. Tel.: +49-30-8413-4132; fax: +49-30-8413-4105.
E-mail address: rupprechter@fhi-berlin.mpg.de (G. Rupprechter).

0039-6028/$ - see front matter © 2004 Elsevier B.V. All rights reserved.
doi:10.1016/j.susc.2004.06.063

Previous reports on Pd(1 1 1) suggested that C–O bond scission is facilitated by near monolayer methanol coverages [1] or by surface defects [4,5]. For Pd–Al_2O_3 model catalysts C–O bond scission during methanol decomposition was reported to preferentially occur on particle steps and edges [6,7]. An increased activity of low-coordinated sites on Rh nanocrystals supported by Al_2O_3 was also observed for hydrocarbon hydrogenolysis [8] and CO dissociation [9].

We have tried to address these issues by studying methanol decomposition both on well-annealed and defect-rich Pd(1 1 1), combining X-ray photoelectron spectroscopy (XPS) and polarization-modulation infrared reflection absorption spectroscopy (PM-IRAS). Ion-bombardment was utilized to create surface defects but it is not clear if the defects generated this way are equivalent to those on nanoparticles. The Pd surfaces were exposed to methanol exposures typical of thermal desorption studies under ultrahigh vacuum (UHV) as well as to an "elevated" methanol background pressure (5×10^{-7} mbar), simulating higher impingement rates. The time- and temperature-dependent evolution of carbonaceous species was studied by XPS, while PM-IRAS was mainly applied to characterize high-pressure (170 mbar) CO structures to elucidate possible sources for carbon deposits.

2. Experimental

The experimental set-up combines a UHV surface analysis chamber with a UHV-high-pressure cell optimised for glancing-incidence PM-IRAS. "Smooth" Pd(1 1 1) was prepared as described in [10] and inspected by low energy electron diffraction (LEED) and XPS (Phoibos 150 using MgKα irradiation with a resolution of $\sim$1 eV). Defect-rich Pd(1 1 1) was prepared by subsequent ion-bombardment (1 keV Ar^+ at 300 K, 5–10 min), and briefly flashed to 500 K to eliminate residual CO and reduce carbon traces below 0.05 ML (carbon had reappeared due to uncovering subsurface carbon by ion erosion). Even after flashing to 500 K the surface remained defective, as indicated by broad LEED reflections and a high background. Methanol (p.a.) was cleaned by freeze-thaw cycles, while CO (99.997%) was purified using a liquid nitrogen cold trap and a carbonyl absorber cartridge.

XPS spectra were acquired in situ during methanol exposure and normalized to the $Pd3d_{5/2}$ integral intensity at 334.9 eV. For PM-IRAS (Bruker IFS66v/S FTIR spectrometer, Hinds-PEM-90 photoelastic modulator), the sample was transferred under UHV to the high-pressure cell (equipped with BaF_2 windows) [10]. PM-IRAS utilizes the polarization modulation of the incident infrared light and is based on the predominance of p- over s-polarized light at a metal surface. Accordingly, the differential reflectance $\Delta R/R$ measured with PM-IRAS represents the surface-specific vibrational spectrum while no gas phase species are detected. For further details about PM-IRAS we refer to [11,12].

3. Results and discussion

Systematic scanning tunneling microscopy (STM) studies of ion-bombarded transition metal surfaces have shown that high ion doses (Ar^+, Ne^+, Xe^+) produced surface defects such as vacancy pits [13,14]. These are the result of the nucleation and growth of vacancy islands inside other previously existing vacancy islands. The morphology of vacancy pits is quite characteristic, with many exposed atomic layers and with a high density of steps and kinks (for STM images see [13]). By comparison with previous work [13,14] we estimate that 5–10 ML of Pd are removed by the ion bombardment and that $\sim$50% of the surface atoms can be considered as defect sites. In a previous SFG study of CO adsorption on sputtered Pd(1 1 1) [10], the surface defects produced an additional CO binding site ($\sim$1990 cm^{-1}) which was not observed on well-annealed Pd(1 1 1). Since annealing to $\sim$600 K was necessary to fully remove the defects, the defects are stable under the conditions applied here.

Fig. 1 shows XPS spectra acquired after adsorbing 15 L (langmuir; 10^{-6} Torr s) CH_3OH on ion-bombarded Pd(1 1 1) at 100 K. As mentioned before, trace amounts of carbon were present on

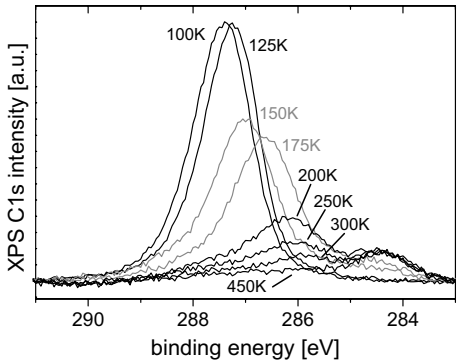

Fig. 1. XPS C1s core-level spectra measured during CH_3OH desorption between 100 and 450 K (exposure: 15 L CH_3OH at 100 K).

the sputtered surface but should be negligible since their concentration is much smaller than that of surface defects. XPS spectra were then acquired at increasing temperature. Their interpretation was aided by temperature-programmed desorption (TPD) (not shown; see e.g. [1]) and by previous XPS studies on Pd(1 1 1). TPD indicated desorption maxima at ~140 and ~175 K for CH_3OH multilayer and CH_3OH monolayer desorption, respectively.

We first discuss C1s signals around 286 eV, which may originate from CH_3OH, CH_xO ($x = 3$–1) and CO. At 100 K, a multilayer of CH_3OH is present, producing a single C1s peak with a binding energy (BE) of 287.4 eV. At this point, no Pd signal was observed, i.e. only the uppermost CH_3OH layers contributed to the XPS spectrum. At 125 K, the multilayer partially desorbed, as indicated by the small shift to 287.3 eV, and the appearance of a very small Pd3d signal. Upon increasing the temperature to 150 K, the CH_3OH multilayer desorbed and ~1 ML CH_3OH remained (as indicated by a strong reduction of the C1s intensity, a shift to 287.0 eV and the clear appearance of Pd3d signals). Further increasing the temperature to 175 K slightly reduced the C1s signal (coverage ≈0.9 ML assuming no changes in the C1s sensitivity factor) but the BE was shifted to 286.6 eV. Based on previous XPS and secondary ion mass spectrometry (SIMS) studies on "smooth" Pd(1 1 1) [1,4] this indicates the onset of CH_3O (methoxy) formation by O–H bond scission. At 200, 250 and 300 K the C1s intensity further decreased (0.6–0.3 ML) and the BE shifted to 286.2, 286.1 and 286.0 eV, respectively. Several processes occur simultaneously between 200 and 400 K: methanol desorption, dehydrogenation of CH_3O via CH_xO to CO, and partial desorption of CO. The 286.0 eV peak at 300 K is due to CO and CH_xO (~0.2 ML). At 450 K, the C1s signal around 286 eV nearly vanished due to CO desorption.

We now focus on the small C1s signals around 284.4 eV which appeared in the spectra between 150 and 450 K. A BE of 284.4 eV is typical of carbon but hydrocarbon species (CH_x; $x = 3$–1) cannot be ruled out. When compared to the (fresh) ion-bombarded surface prior to CH_3OH exposure, only a small (≈0.05 ML) increase of carbon or CH_x was detected. This indicates that methanolic C–O bond scission is very limited under the applied conditions and that CH_3OH desorption and dehydrogenation dominate. At ~700 K the signal at 284.4 eV fully disappeared due to carbon dissolution in the Pd bulk. However, most importantly, a very similar result was obtained for CH_3OH desorption/decomposition on well-annealed Pd(1 1 1) indicating that C–O bond scission was not considerably enhanced by surface defects.

Since C–O bond scission should be facilitated at higher temperature, experiments were also carried out at 300 K, exposing the Pd surfaces to 5×10^{-7} mbar CH_3OH. Fig. 2 compares XPS spectra of well-annealed and defect-rich Pd(1 1 1) taken after 80 min of CH_3OH exposure. In both cases two

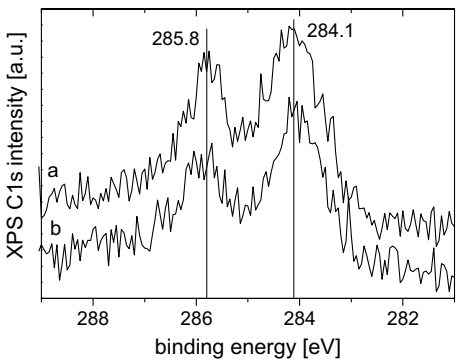

Fig. 2. XPS C1s core-level spectra measured after exposing well-annealed (a) and ion-bombarded (b) Pd(1 1 1) to 5×10^{-7} mbar CH_3OH for 80 min (300 K).

peaks were observed, at 285.8 eV due to CO and CH_xO and at 284.1 eV due to carbon or carbonaceous species (≈0.3 ML). Apparently, under these conditions a higher (total) amount of C–O bond scission takes place but it is again found independent of surface structure.

Fig. 3a compares the time-dependent signal intensity of carbonaceous species on the two surfaces. On the timescale studied, both for perfect and defect-rich Pd(1 1 1) the rate of CH_x ($x = 0$–3) formation is very similar, except from an "offset", i.e. the carbon initially present on the sputtered surface (as described above). Fig. 3b shows the evolution of the BE of the carbonaceous species with time. On the perfect (1 1 1) surface the BE shifted from 283.8 to 284.05 eV and, according to a study by Rodriguez et al. [15], can be interpreted as a transition from isolated carbon atoms to carbon clusters. This suggests that on perfect Pd(1 1 1) isolated carbon atoms initially result from C–O bond scission which then act as nucleation centers for subsequently produced carbon atoms (diffusing over the surface), finally leading to carbon clusters (hydrocarbon fragments cannot be excluded though). By contrast, on the sputtered surface small carbon clusters are already present from the beginning and subsequent carbon deposition increases the amount of carbonaceous species but does not shift the binding energy (Fig. 3b).

Summarizing, in agreement with previous studies we confirm that under typical UHV conditions C–O bond scission is only a very minor path in CH_3OH decomposition on well-annealed Pd(1 1 1) (e.g. [1]). In addition, we find that surface defects created by ion-bombardment do not enhance C–O bond scission. Catalyst deactivation is hence not an issue under UHV conditions. If the CH_3OH pressure is raised to 5×10^{-7} mbar at 300 K, carbon deposition becomes considerable, which poisons the catalyst and limits the usefulness of CH_3OH decomposition as hydrogen source. However, also at that pressure C–O bond scission was not significantly enhanced by surface defects. With respect to previous studies on Pd–Al_2O_3 [6] it appears that the behavior of step and edge sites on Pd nanoparticles (which exhibited an increased C–O bond scission activity) is not mimicked by sputter-induced defects.

Because XPS cannot fully differentiate between CH_3OH, CH_xO and CO (at least with the resolution of our X-ray gun), further experiments were carried out using infrared spectroscopy. Fig. 4 shows a PM-IRAS spectrum of 6 L CH_3OH on Pd(1 1 1), with typical bands at 2830 cm^{-1} (νCH_3), 1455 cm^{-1} (δCH_3), 1130 cm^{-1} (ρCH_3), and 1045

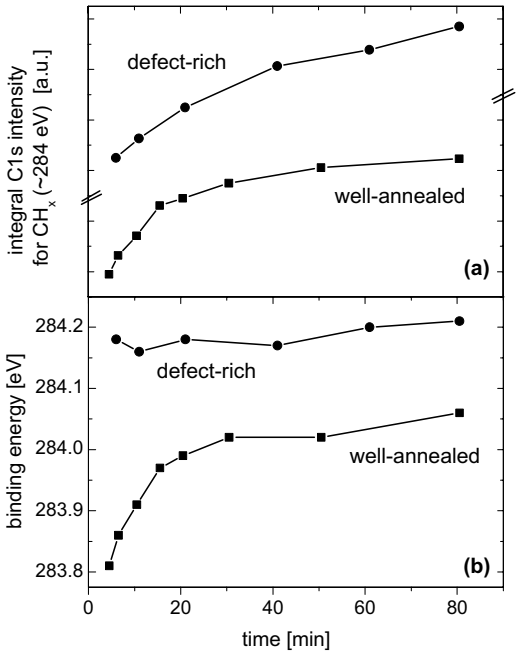

Fig. 3. Time-evolution of the integral intensity of carbonaceous species (a) and of their C1s binding energy (b), both for well-annealed and defect-rich Pd(1 1 1); see text.

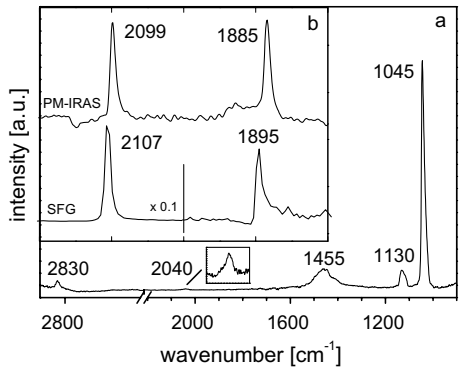

Fig. 4. (a) PM-IRAS spectrum of 6 L CH_3OH on Pd(1 1 1) at 100 K. (b) PM-IRAS and SFG spectra of 170 mbar and 100 mbar CO on Pd(1 1 1) at 190 K, respectively.

cm^{-1} (νCO). A very small CO signal was observed, which rather originates from residual CO than from CH_3OH decomposition [1,16]. With increasing temperature, the CH_3OH bands vanished, again suggesting that desorption dominated over dehydrogenation (and C–O bond scission) under UHV. Experiments at higher pressures of $\sim 10^{-6}$ mbar (corresponding to Fig. 2) are in progress.

Another question related to carbon deposits is their origin, i.e. do carbon(aceous) species directly originate from CH_3OH (via CH_xO [4] or dehydration [1,3]) or are they due to dissociation of the decomposition product CO? CO dissociation was, for instance, reported for Pd nanoparticles and for sputtered Pd foil [17]. In order to investigate this question we have exposed up to 170 mbar CO at 190 K, monitoring the adsorbate layer with PM-IRAS. As mentioned above, PM-IRAS allows to selectively probe adsorbed CO while gas phase contributions can be removed. Fig. 4b displays a PM-IRAS spectrum of 170 mbar CO on well-annealed Pd(1 1 1) at 190 K, typical of a (2×2) structure with hollow (1885 cm^{-1}) and on-top (2099 cm^{-1}) bonded CO (≈0.75 ML). This structure is in good agreement with our previous high-pressure SFG studies [10] and an SFG spectrum of 100 mbar CO is shown for comparison. The offset in frequency can be explained by different contributions of CO domains with slightly lower coverage (influencing the size of (2×2) domains), as described in [18]. No indications of CO dissociation (such as strong frequency shifts or a reduction of signal intensity with time due to carbon deposition) were observed even after hours of high-pressure CO exposure. SFG/XPS studies on Pd(1 1 1) up to 1000 mbar and 400 K did also not detect carbon deposits [10,19]. Consequently, carbonaceous species must originate directly from CH_3OH/CH_xO precursors and not from dissociation of the decomposition product CO.

4. Conclusions

CH_3OH desorption/decomposition on well-annealed and defect-rich Pd(1 1 1) was studied by XPS and PM-IRAS. Under UHV, C–O bond scission was very limited and independent of surface structure, while after exposing CH_3OH at 5×10^{-7} mbar and 300 K ≈0.3 ML carbonaceous deposits (CH_x; $x = 0$–3) were detected on both surfaces. The rate of CH_x formation, however, was very similar on well-annealed and defect-rich Pd(1 1 1), indicating no considerable influence of surface defects generated by ion-bombardment on C–O bond scission. It seems that defects generated by ion-bombardment do not exhibit the high C–O bond scission activity of steps and edges on Pd nanoparticles. On well-annealed Pd(1 1 1) carbon deposition proceeded from isolated carbon atoms to carbon clusters. PM-IRAS allowed us to study high-pressure CO adsorption and to exclude the possibility of CO dissociation on both surfaces. Accordingly, carbonaceous species observed during CH_3OH decomposition must originate from CH_3OH/CH_xO precursors. To investigate the influence and nature of defects in more detail, future time-dependent XPS and high-pressure PM-IRAS experiments of methanol decomposition on oxide supported Pd nanoparticles are crucial.

Acknowledgements

Part of this work was supported by the German Science Foundation (DFG) through priority program SPP1091. ORdF is grateful for a Humboldt fellowship.

References

[1] J.-J. Chen, Z.-C. Jiang, Y. Zhou, B.R. Chakraborty, N. Winograd, Surf. Sci. 328 (1995) 248.
[2] C.J. Zhang, P. Hu, J. Chem. Phys. 115 (2001) 7182.
[3] R. Schennach, A. Eichler, K.D. Rendulic, J. Phys. Chem. B 107 (2003) 2552.
[4] M. Rebholz, N. Kruse, J. Chem. Phys. 95 (1991) 7745.
[5] M. Mavrikakis, M. Barteau, J. Molec. Catal. A 131 (1998) 135.
[6] S. Schauermann, J. Hoffmann, V. Johánek, J. Hartmann, J. Libuda, H.-J. Freund, Catal. Lett. 84 (2002) 209.
[7] H.-J. Freund, M. Bäumer, J. Libuda, T. Risse, G. Rupprechter, S. Shaikhutdinov, J. Catal. 216 (2003) 223.
[8] G. Rupprechter, G. Seeber, H. Goller, K. Hayek, J. Catal. 186 (1999) 201.
[9] M. Bäumer, H.-J. Freund, Prog. Surf. Sci. 61 (1999) 127.

[10] G. Rupprechter, H. Unterhalt, M. Morkel, P. Galletto, L. Hu, H.-J. Freund, Surf. Sci. 502–503 (2002) 109.
[11] G.A. Beitel, A. Laskov, H. Oosterbeek, E.W. Kuipers, J. Phys. Chem. 100 (1996) 12494.
[12] (a) E. Ozensoy, D. Meier, D. Goodman, J. Phys. Chem. B 106 (2002) 9367;
(b) Y. Jugnet, F.J. Cadete Santos Aires, C. Deranlot, L. Piccolo, J.C. Bertolini, Surf. Sci. 521 (2002) L639.
[13] M. Kalff, G. Comsa, T. Michely, Surf. Sci. 486 (2001) 103.
[14] O. Rodríguez de la Fuente, M.A. González, J.M. Rojo, Phys. Rev. B 63 (2001) 085420.
[15] N.M. Rodriguez, P.E. Anderson, A. Wootsch, U. Wild, R. Schlögl, Z. Paal, J. Catal. 197 (2001) 365.
[16] H. Lüth, G.W. Rubloff, W.D. Grobmann, Surf. Sci. 63 (1977) 325.
[17] V. Matolín, I. Stará, N. Tsud, V. Johánek, Progr. Surf. Sci. 67 (2001) 167.
[18] M. Morkel, H. Unterhalt, M. Salmeron, G. Rupprechter, H.-J. Freund, Surf. Sci. 532–535 (2003) 103.
[19] V.V. Kaichev, I.P. Prosvirin, V.I. Bukhtiyarov, H. Unterhalt, G. Rupprechter, H.-J. Freund, J. Phys. Chem. B 107 (2003) 3522.